

Muon measurement with an ice Cherenkov tank at the South Pole

X. Bai¹, T. K. Gaisser¹, A. Karle², Z. Ma³, K. Rawlins², G. M. Spiczak¹, and T. Stanev¹

¹Bartol Research Institute, Univ. of Delaware, Newark, DE 19716, USA

²Department of Physics, Univ. of Wisconsin, Madison, WI 53706, USA

³Physics Department, Univ. of Delaware, Newark, DE 19716, USA

Abstract. A 1.4 m^3 ice Cherenkov tank was installed at the South Pole during the 2000-2001 austral summer. The penetrating muon rate was measured for three different incident angles with a scintillator muon telescope incorporating the tank as absorber. The freezing process was monitored and the detector was calibrated with the penetrating muons. The calibration is compared to a GEANT simulation of the detector. Signals coincident with air showers have also been recorded using a trigger from the surrounding SPASE-2 (South Pole Air Shower Experiment-2) array.

1 Introduction and Motivation

Water Cherenkov detectors have been used as the primary detector elements in the Haverah Park surface array (Lawrence *et al.*, 1991) and in the current Auger engineering detector (Auger Project, 1996). The idea of a frozen version of the Cherenkov tank as a component of an air shower array was first tested by Barwick and Beaman in 1991/92 within the SPASE-1 (South Pole Air Shower Experiment-1) array. In that test twenty bare photomultipliers were placed in the bottom of a commercial swimming pool that was gradually filled with water allowed to freeze layer by layer. After several months ten photomultipliers survived, and a test in which the pool was triggered by SPASE-1 showed that in 70% of all events all of these photomultipliers gave a signal. For these events a timing resolution of 1.8 ± 0.2 ns was demonstrated (Barwick & Beaman, 1993).

Since 1996 the new SPASE-2 array has been operating in coincidence with the AMANDA (Antarctic Muon And Neutrino Detector Array) neutrino telescope, as reported elsewhere at this conference (Bai *et al.*, 2001). In anticipation of future growth of a neutrino observatory in the Antarctic ice sheet, we decided to perform another test of a frozen Cherenkov detector as an element of an air shower array, this time using AMANDA optical modules (OMs) (Andres *et al.*,

2001) to obtain the signal from the tank. We also took the opportunity to make a controlled and precise measurement of the flux of muons at the South Pole altitude ($\sim 700\text{g}/\text{cm}^2$). This measurement is of interest as a calibration point for calculations of atmospheric neutrinos, as described in another contribution to this conference (Engel *et al.*, 2001).

2 Details of Deployment

The test detector is a cylindrical polyethylene tank of $1.14\text{m}^2 \times 1.24\text{m}$ installed at the South Pole inside the boundary of the SPASE-2 array (Dickinson *et al.*, 2000). The inside of the tank is lined with white, diffuse-reflecting Tyvek type 1025D. The exterior of the tank was wrapped in a layer of insulation to keep the freezing process slow, so it could be observed. After filling with station drinking water, two AMANDA OMs, with a separation of 51cm , were mounted face down symmetrically off-center with their photocathode region completely submerged. A $1.6\text{cm} \times 89\text{cm}$ cartridge heater was immersed down the center of the tank. The power sent to the heater ($\sim 950\text{W}$ maximum at 110V) was adjustable and reduced gradually to the minimum required to maintain an open water channel that allowed room for expansion and for air bubbles to escape the freezing front producing fairly clear ice. The entire freezing process took 36 days with the outside temperature averaging around -28°C with little freezing during the first 14 days.

A muon telescope consisting of three 0.2m^2 scintillators, two stacked on top of the tank and one underneath, identifies penetrating muons for calibration. After the tank was frozen, the heater was removed and the top ice surface was covered with a layer of black velvet. The resulting ice depth was 99.1cm . A sketch of the detector is shown in figure 1. Signals from the two OMs and the scintillators are transmitted through $\sim 100\text{m}$ of twisted pair and RG-8 coaxial cables, respectively, to the central SPASE-2 building that houses the electronics and data acquisition. Waveforms are recorded from a 1GHz Tektronix digital oscilloscope with a Linux PC

through the PCI-GPIB interface.

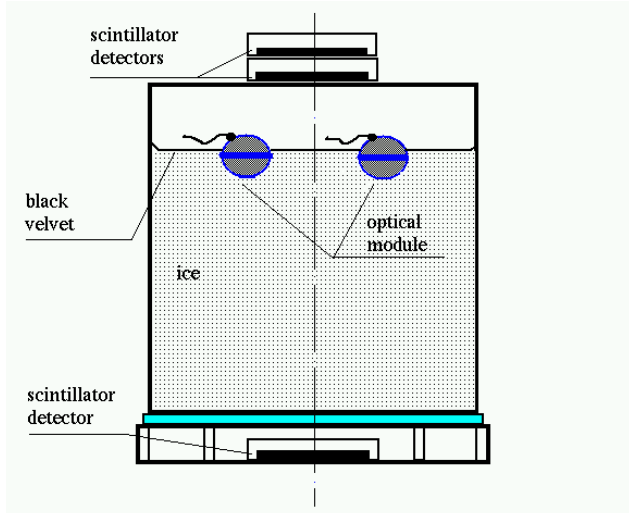


Fig. 1. A sketch of the ice Cherenkov detector.

3 Monitoring Response with Vertical Penetrating Muons

Since penetrating muons deposit a characteristic amount of Cherenkov light per radiation length in the medium, the background cosmic ray muons selected by a muon telescope are used for detector calibration and monitoring.

3.1 Single Penetrating Muon Waveforms and Simulation

The measured vertical penetrating muon waveform (averaged over 500 muons) is compared with an averaged GEANT simulation waveform as seen at the top in figure 2. In the simulation, we represented one photoelectron (PE) as a Gaussian with $\sigma = 12.0ns$. The width was estimated with the oscilloscope traces, however the shape is not exactly Gaussian. We propagate the photons with a diffusive reflection on Tyvek surfaces and track them in the water using the standard photon absorption length for clear water of $82.0m$ which varies by a factor of 0.092 to 1.0 depending on wavelength.

The risetime profile and amplitude seen in the data agrees fairly well with the simulation. However, the falltime profile of the true waveform does not agree well with the simulation because the bases of the OMs we are using are designed to give a slow decay for AMANDA, which is not included in the present simulation.

A simplified method was also applied to estimate the average number of PEs for a single penetrating muon. By using equation (Ravignani *et al.*, 1997):

$$\left(\frac{\sigma}{\mu}\right)_{exp}^2 = \frac{1 + \left(\frac{\sigma}{\mu}\right)_{se}^2}{\langle PE \rangle} + \left(\frac{\sigma}{\mu}\right)_{light}^2 \quad (1)$$

and borrowing the values of the parameters from this reference, we estimate > 41 PEs from the charge spectrum at the bottom of figure 2. One of the main uncertainties comes

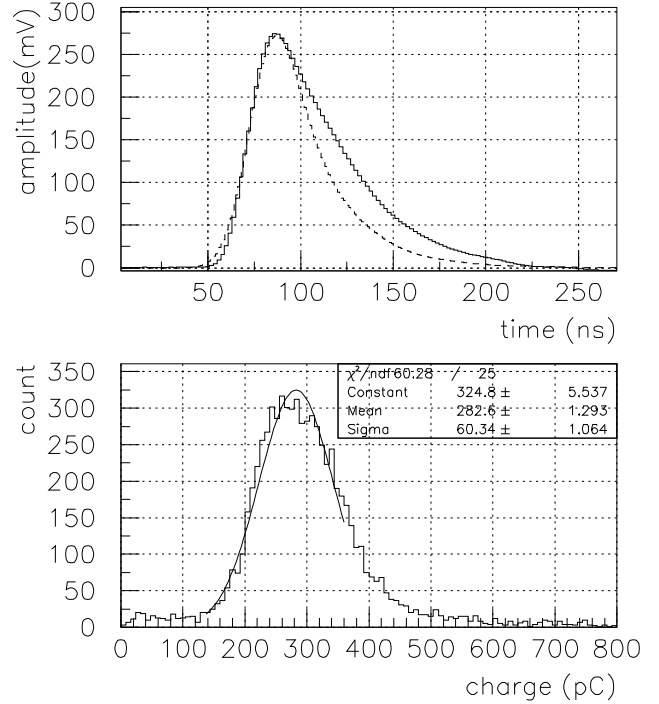


Fig. 2. Top: Vertical average penetrating muon waveform (solid line) and comparison with a GEANT simulation (dashed line). Bottom: Charge spectrum obtained by integrating several first day waveforms.

from the fact that we have a larger Cherenkov light dispersion by using $0.2m^2$ scintillators for the muon telescope (thus slightly non-vertical showers). Term $\left(\frac{\sigma}{\mu}\right)_{se}$ in (1) is also expected to be different in our case because the OMs and bases used are somewhat different than the bare photomultiplier tube used for the study by Ravignani *et al.* (1997). All these will increase the estimated number of photoelectrons generated in our detector. The precise values of these parameters needed for a more accurate estimation will be determined with future work.

3.2 Time Dependence as Seen by Vertical Penetrating Muon Signals

After the tank was filled with water, the time dependence of the signal was monitored using vertical penetrating muons. The muon waveforms were continuously recorded by the digital oscilloscope except for short down times required for visual checks. Three parameters of vertical penetrating muon signals were used to monitor the freezing process and stability: signal amplitude, integrated charge and effective decay time. Figure 3 shows the variation of these parameters. We can see that signals changed significantly when the water first began to freeze, as shown from period 1 to 2, likely due to the changing optics of the system. Then, both the amplitude and charge increased as more water froze during period 2. The freezing rate steadily decreased as the increasing amount of surrounding ice provided additional insulation. Thus, period

3 corresponds to an effort to speed up the freezing rate by uncovering the tank and removing the surrounding insulation. We noticed a crack developed in the ice during this period. The tank was closed up after period 3. A noticeable sudden change in decay time, amplitude and charge happened in period 4. This is believed to be caused by the appearance of a new crack in the ice when the small amount of remaining slush froze after removal of the heating rod. The ice will be visually checked for such cracks and other qualities in the coming season. Before the tank was sealed, the ice surface was smoothed and covered with a sheet of black velvet to absorb light reaching the top to reduce further bounces within the tank that tend to stretch out the time structure of the signals. We also notice a $\sim 20\%$ increase in the amplitude of the signal during the 100 days since the tank was closed up. The reason is so far not understood, though it could be due to gradual settling down of the OMs as the temperature decreases and they are kept in darkness. This amplitude increase does not result in much increase in the signal charge because it is essentially offset by a $\sim 4ns$ decline in the signal FWHM.

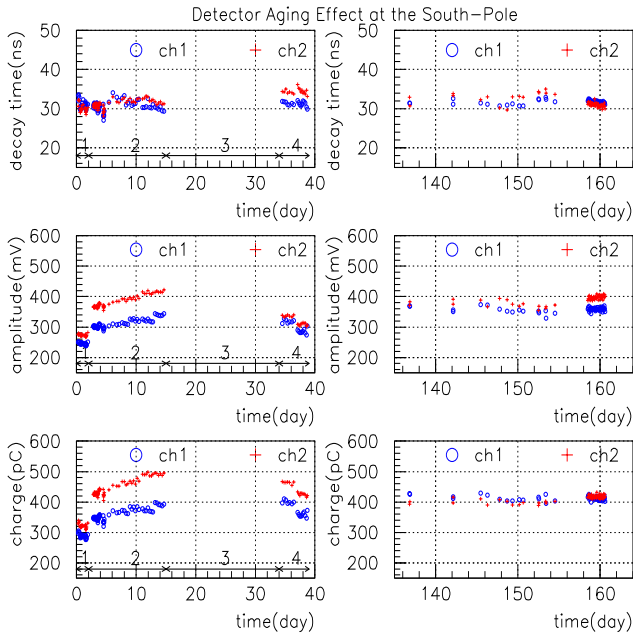


Fig. 3. Time dependence measured by the effective decay time (top), signal amplitude (middle) and integrated charge (bottom). The four marked periods are: 1-all liquid water; 2- $\sim 20\%$ frozen; 3-tank open to increase freezing rate; 4-almost completely frozen with small volume of slush at the center. Right hand plots are from data recorded 100 days later by our winter overs after the temperature has declined by about 30° C or more.

Despite these uncertainties, it is promising that the detector response has not changed significantly more than 3 months after freezing. Monitoring will continue throughout the year.

4 Penetrating Muon Rate at the South Pole

The penetrating muon rate at the South Pole measured at three different zenith angles (θ) is summarized in column one of table 1. Only the statistical errors are given. Column two gives the acceptances of the muon telescope at these three zenith angles. These numbers are obtained by a Monte Carlo simulation that required 1.0×10^4 particles to pass through all three scintillators for each case. The last two columns show the integrated fluxes and the minimum kinetic energy of the muons able to pass through all the three scintillators, respectively.

Table 1. Penetrating muon rate and flux at the South Pole. The muon energy loss table for the minimum penetrating kinetic energy calculation is from <http://pdg.lbl.gov/~deg/muon.html> (Groom *et al.*, 2001)

θ $^\circ$	rate Hz	acceptance $(m^2 \cdot sr)^{-1}$	integrated flux $(s \cdot m^2 \cdot sr)^{-1}$	E_{min} MeV
0	2.22 ± 0.01	1.22×10^{-2}	182 ± 1	246.0
15	1.80 ± 0.01	1.02×10^{-2}	176 ± 1	263.5
35	0.72 ± 0.01	4.87×10^{-3}	148 ± 2	311.7

A Monte Carlo simulation was carried out for the muon fluxes expected for the average atmosphere depth of $702g/cm^2$ during the muon measurement. The simulation used TARGET2.1 (Engel *et al.*, 2001) and the cosmic ray flux derived by Agrawal *et al.* (1996) for the epoch of solar maximum. Muon fluxes of 180, 173 and $168 (s \cdot m^2 \cdot sr)^{-1}$ were predicted for the three angles. The measured nearly vertical muon fluxes are in excellent agreement with the prediction, while at 35° it is lower by 12%.

5 Ice Cherenkov Signal Coincident with Air Showers

The detector was also triggered by the SPASE-2 shower array to study how its signal changes with the shower size and distance from the shower core. In order to include nearby shower signals and large shower signals, one of the OMs was run at high gain with the high voltage of 1100V (ch 1) and the other was run at low gain using 900V (ch 2). Profile plots corresponding to four different core distance bins, 5–20m, 20–35m, 35–50m and 50–65m are shown in figure 4. The vertical equivalent muon density in the scintillator at 30m from the shower core, S_{30} , is a measure of the size of the shower as reconstructed in SPASE data analysis.

For the present setup, the waveform amplitude saturates at 2.0V for the high gain channel and 1.0V for the low gain channel as determined from large nearby showers. It is shown in figure 4 that when one samples a shower close enough to the shower core the high gain channel saturates for relatively small showers (top left entry), while the low gain channel shows no sign of saturation (top right entry). At intermediate core distances the high gain channel still saturates for showers with larger S_{30} . However, the high gain channel rarely saturates when it is far from the core (bottom left en-

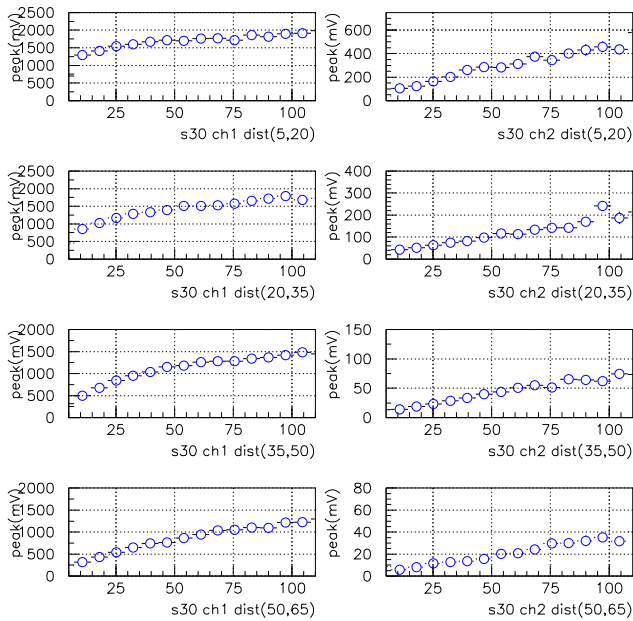


Fig. 4. Lefthand set of figures show the response of the high gain OM, and the righthand - of the low gain OM, as a function of S_{30} for different shower core distance bins. See text for a more detailed explanation.

try). These features are also seen when looking at the individual waveforms. This suggests one method for ensuring a large dynamic range that is needed to cover a large shower energy range in a future experiment.

6 Remarks and Summary

The construction and test of this ice Cherenkov detector shows that it is practical to develop such an instrument for air shower detectors at the South Pole. The extreme weather conditions, however, require more studies on the construction of large tanks or producing large volumes of clear ice on site. We also have to study different possible freezing techniques and investigate how potential cracks may affect the detector uni-

formity. An alternative to the heating rod could be a freezing technique that involves introduction of bubbles in the center of the tank that keep a liquid channel all through the freezing. We remind the reader that because of the small dimensions of the tank compared to the underground detector, and the requirement to have diffuse light, the quality of the detector would not be decreased by a small amount of bubbles. To fully prepare for a final design of the detector we have to investigate all these questions and to solve the related engineering work problems.

We are planning to continue the monitoring of the tank described here and to inspect visually the ice quality during the next austral season. At that time we plan to build a full size ($7 m^2$) detector and perform additional studies on freezing techniques, calibration, background and shower signals. We will also attempt to equip the tank with digital OMs and test a new data acquisition system.

Acknowledgements. The work is support by a grant from the Office of Polar Programs of the U.S. National Science Foundation. The authors also appreciate the support from the U.S. Amundsen-Scott South Pole station, AMANDA winterover personnel and a special thanks to Jerry Poirier for all of his assistance.

References

- V.Agrawal et al. Phys Rev D53(1996)1314.
- E.Andres et al. Nature 410(2001)441.
- Pierre Auger Observatory, <http://www.auger.org>
- X.Bai et al. "Calibration and Survey of AMANDA with SPASE", this conference.
- S.Barwick and J.Beaman, 1993, Proc.23rd Int.Cos.Ray Conf. (Calgary),4,683.
- J.E.Dickinson et al. NIM 440(2000)95.
- Ralph Engel, Thomas K. Gaisser and Todor Stanev, this conference.
- D.E.Groom, N.V.Mokhov, and S.I.Striganov, <http://pdg.lbl.gov/~deg/muon.html>
- M.A.Lawrence,R.J.O.Reid and A.A.Watson, J.Phys. G17(1991)733.
- D.Ravignani et al. Pierre Auger Observatory Technical Note, GAP-97-024 http://www.auger.org/admin/GAP_Notes/